https://doi.org/10.22226/2410-3535-2023-1-3-8

Signs of the presence of an ordered phase in the Cu-5.9 at.% Pd alloy after its long-term annealing at a moderate temperature

O. S. Novikova†, A. E. Kostina, E. G. Volkova, Yu. A. Salamatov, A. V. Glukhov, A. Yu. Volkov, V. V. Marchenkov, V. S. Gaviko, Yu. M. Ustyugov

†novikova@imp.uran.ru

M. N. Mikheev Institute of Metal Physics, UB of RAS, Ekaterinburg, 620108, Russia

The structure and electrical properties of the Cu-5.9 at.% Pd alloy were studied after its annealing for two months at 250°C. As a result of such a long-term thermal treatment, in the XRD patterns taken from the alloy one can observe a weak superstructural (100) reflection, which seems abnormal, since the alloy can only be in the state of a disordered single-phase solid solution (as it follows from the generally accepted Cu-Pd phase diagram). Quantitative analysis of the X-ray diffraction patterns reveals the presence of two new phases with different contents of Pd. An assumption is made that $L1_2$ superstructure can be formed in the Pd-enriched phase. The specific features observed in the temperature dependence of electrical resistivity, as well as the TEM results, confirm this set-forth hypothesis of ours. Using the resistometric method, the temperature of the order-disorder phase transition in the alloy was estimated as $T_c \approx 340$°C. It is concluded that the position of the A1-(A1+$L1_2$) phase boundary in the Cu-Pd phase diagram requires more precise definition in the region of compositions on the side of the low Pd content.

Keywords: Cu-Pd phase diagram, dilute Cu-Pd alloys, $L1_2$ superstructure, resistometric study, microstructure.

1. Introduction

Cu-Pd alloys are interesting for many promising applications. For example, Cu-Pd alloys of a near equiatomic composition are efficient catalysts, and are used to produce membranes for H_2 purification [1–5]. Cu-based alloys with a low Pd-content feature a good combination of high strength and corrosion resistance [6,7]. In order to effectively improve the properties of these materials, it is important to know the accurate phase diagram of the Cu-Pd system [1,8].

As is known, two types of ordered phases occur in this system [9]. During slow cooling of the Cu-Pd alloys of a near equiatomic composition, their disordered fcc solid solution transforms to the ordered B2-type structure. In turn, the ordered $L1_2$-type phase exists in the alloys around Cu_3Pd stoichiometry. There are currently two known versions of the Cu-Pd phase diagram plotted by different researchers for these dilute alloys [9,10]. As follows from [9], the disordered fcc solid solution is formed in Cu-Pd alloys if Pd-concentration in them is below ≈8 at.% (Fig. 1).

The phase diagram in [10] was only built for alloys containing more than 10 at.% of Pd. It should be noted that both the versions have almost no experimental points in their areas with low Pd content. It was concluded [11] that the position of the low temperature branches of the temperature-concentration boundaries of the phase transitions in the Cu-Pd alloys are not fully established yet.

Earlier [6,12], we have studied the structure, physical and mechanical properties of Cu-Pd alloys containing from 0 to 8.0 at.% Pd. Under the thermal treatments, the behavior of the alloys with low Pd-content (less 4.6 at.% Pd) was found to be the same as that of pure Cu. It was concluded that a single-phase fcc solid solution is formed in these alloys. However, it was discovered the increasing of electrical resistivity and microhardness in the course of annealing of the Cu-4.6 Pd and Cu-5.9 Pd alloys (here and further, for the sake of brevity, we will omit 'at.%' in the alloy names). The annealing hardening has also been observed before in the Cu-7 Pd alloy [13]. It was very difficult for authors of this work to

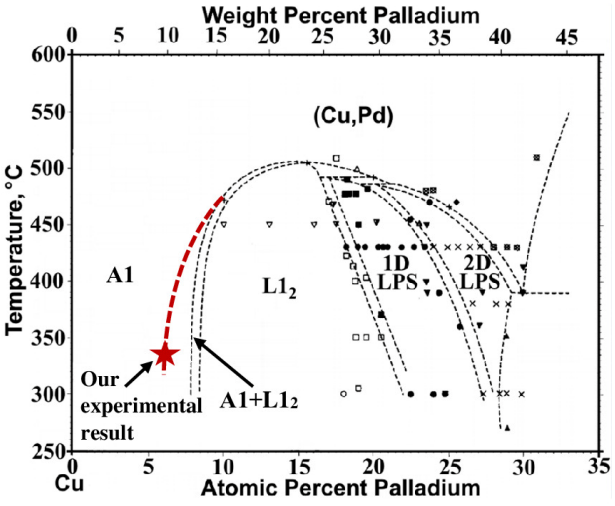

Fig. 1. (Color online) The part of the Cu-Pd phase diagram in the vicinity of the Cu_3Pd stoichiometry plotted in work [9]. The sign "★" marks the temperature boundary of the A1↔(A1+$L1_2$) phase transition of the Cu-5.9 Pd alloy that was determined in this study.

explain the discovered effect based on the generally accepted Cu-Pd phase diagram and considering the Cu-7 Pd alloy as a single-phase one. Rather, this behavior would be typical of the formation of the 2nd phase nuclei in the alloys [14]. Indeed, the abnormal thermal dependences of the electrical resistivity and microhardness are observed in the Cu-8 Pd alloy with two-phase ($A1+L1_2$) structure [15]. Moreover, from an *ab initio* electronic structure calculation, which had been conducted in [16], it was predicted the disorder-order ($A1-L1_2$) transition in the Cu-7Pd alloy. As follows from the model calculations performed in [17,18], the ordered $L1_2$ phase can be formed even in the Cu-5 Pd alloy. On the whole, results of experimental studies [12,13] and model calculation data [16–18] give reasons to believe that the two-phase ($A1+L1_2$) region in the Cu-Pd phase diagram is somewhat wider than it is drawn in Fig. 1.

It was concluded in [11,19] that it is very difficult to accurately determine the phase boundaries in the Cu-Pd system at moderate temperatures due to extremely low transformation rate and a small fraction of new phase. It requires using both long-term heat treatments and theoretical predictions in the scientific researches (such approach was made in [1, 20, 21], for example). Indeed, the temperature-concentration boundaries are absent below 300°C in Fig. 1.

The aim of our work is to study the structure and properties evolution during long-term annealing of the Cu-5.9 Pd alloy at a moderate temperature.

2. Materials and experimental methods

The Cu-5.9 Pd alloy was prepared by melting of palladium and copper of 99.98% and 99.95% purity, respectively. The melting was performed in the vacuum of at least 10^{-2} Pa, and the alloy melt was poured into a graphite crucible. The chemical composition of the alloy samples was analyzed using a JEOL JCXA-733 microprobe instrument.

A ∅5-mm ingot was homogenized at 800°C for 3 hours and was cut then into two pieces. One piece of the ingot was drawn at ambient temperature to obtain ∅0.22-mm thin wire (for resistometric study). Another piece of the ingot was rolled at room temperature to obtain (i) 0.3-mm thick plates (for X-ray analysis) and (ii) 100-μm thick foils (for TEM investigations). All these specimens were annealed at 800°C for 1 h with the following quenching in cold salt water. It should be emphasized that we studied in our work the structure and properties evolution of the sample alloy which were only in the previously quenched state. A long-term annealing of the pre-quenched specimens was performed at 250°C for 2 months. All heat treatments were carried out on the specimens in evacuated quartz or glass ampoules.

The specific electrical resistivity was measured by the four-point method using the direct electric current of 20 mA. The temperature dependences of the electrical resistivity were measured starting from the liquid nitrogen temperature to just 580°C, under a pressure of about 1×10^{-3} Pa; the rates of heating and cooling of the specimens were 120 K/hour. X-ray structural study was carried out using a high-resolution diffractometer "Empyrean" in copper filtered CuK_α radiation. A JEM-200CX transmission electron microscope (TEM) was used to examine the microstructure of the alloy.

3. Results

As seen in Fig. 1, in the Cu-Pd diagrams there are no experimental points both in the composition area where palladium content is below 10 at.% and in the temperature intervals below 300°C. It means that there are extremely few studies dedicated to investigation of the structure and properties of the dilute Cu-Pd alloys. Below we will describe the results of studies of the structure and properties of the Cu-5.9 Pd alloy samples, which were subjected to annealing at 250°C for 2 months.

Figure 2 shows an XRD diffractogram for the case of this long-term annealed alloy. Very narrow XRD peaks of high intensity are the indication of a nearly equilibrium state in the specimen. At first glance, it seems that this diffractogram contains only fundamental fcc peaks.

In order to analyze the shape of the peaks, the deconvolution via regularization method described in [22] was used. The instrumental function has a pseudo-Voigt profile with equal average-weighted coefficients for Gaussian and Lorentzian components. The result of the quantitative analysis is demonstrated in Fig. 3. One can see in Fig. 3 a that the (111) peak for the annealed alloy consists of two central peaks of a higher intensity and two peaks of lower intensity on the right and left from them. The convolution of these peaks with instrumental function is in good agreement with the initial experimental peak (Fig. 3 b).

Calculations of the lattice parameter based on the central $K\alpha_1$ and $K\alpha_2$ lines have given the same result: $a \approx 3.640$ Å. This is virtually the same, as the lattice parameter in the case of the quenched Cu-5.9 Pd alloy is $a = 3.639$ Å. The values of lattice parameters of the two new phases, to which the smaller peaks in Fig. 3 b correspond, were assessed as: $a_1 \approx 3.623$ Å and $a_2 \approx 3.655$ Å. Thus, our quantitative analysis shows that, during the long-term annealing, the Cu-5.9 Pd alloy matrix undergoes decomposition with generating two phases. The result we have obtained is very well substantiated by the previously published data about re-distribution of atoms during low-temperature annealing of Cu-7 Pd alloy [13]. The EDS-scanning of this alloy after deformation followed by annealing at 330°C is shown a strong Pd-segregation along the grain boundaries.

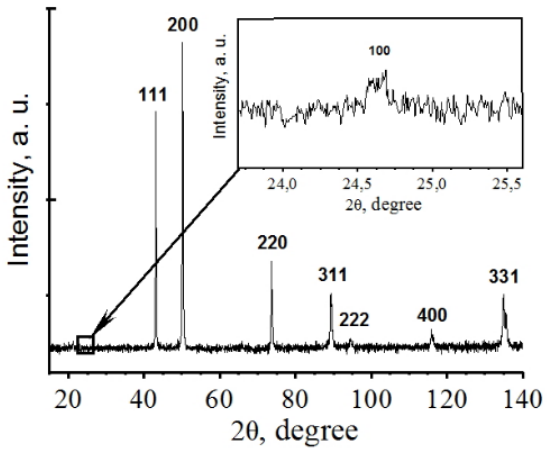

Fig. 2. The XRD results of investigation for the Cu-5.9 Pd alloy annealed at 250°C for 2 months (the insert shows the superstructural (100) peak under a high-resolution mode).

As is known, the variation of the lattice parameters of dilute Cu-Pd alloys with composition is in good correlation with Vegard's law [9]. This enables us to assess compositions of each of the new phases in Fig. 3 a. The phase with the smaller lattice parameter contains ≈2 at.% Pd, whereas the composition of the other phase is near the composition Cu-11Pd. It follows from the Cu-Pd phase diagram that an $L1_2$-type superstructure can be formed in the phase enriched in Pd. Indeed, the weak superstructural (100) peak is directly seen in the regime of a high resolution mode of the diffractometer (see the insert in Fig. 2).

Figure 4 presents the TEM image of a typical microstructure of the Cu-5.9 Pd alloy annealed at 250°C for 2 months. A heterogeneous contrast is observed in the bright-field micrograph (Fig. 4 a), which could well be interpreted as a mark of initial stages of decomposition. Indeed, such a contrast could be the result of concentration variations within the bulk of the material or of small differences of the interplane distance across the foil thickness [15]. The selected area diffraction pattern (SAED) is typical of the fcc crystal structure (see the insert in Fig. 4 a). There are no superstructure reflections in this pattern. However, the dark-field image (Fig. 4 b) shows clearly some very fine particles at the boundary of two grains. One can also note that the shape of this boundary is strongly twisted.

The TEM-result shown in Fig. 5 is of particular interest. There is a round particle seen clearly in the central part of the bright-field image in Fig. 5 a.

The SAED taken from the central part of Fig. 5 a has some weak super-structural reflections (pointed by the arrows in Fig. 5 b). The dark-field image in Fig. 5 c was taken in the reflection of (002) type. Fig. 5 d shows an enlarged view of the central part of the SAED pattern in Fig. 5 b. Some splitting of the fundamental reflections (marked with the arrows in Fig. 5 d) indicates a little variation of the lattice parameter. It can be concluded that this SAED pattern is a result of the superposition of the reflections from two phases. The presence of superstructure reflection of the (001) type in Fig. 5 d indicates unambiguously the formation of an ordered phase in the particle.

Figure 6 shows the temperature dependence of the electrical resistivity of the long-term annealed Cu-5.9 Pd alloy. One can see clearly in Fig. 6 that branches of the dependence diverge notably near 300°C. Moreover, after the heating-cooling cycle, the electrical resistivity of the alloy at cryogenic temperatures become slightly smaller than it was before experiment. These results are in agreement with the annealing behavior of the dilute Cu-Pd alloys with $L1_2$ superstructure [23 – 25]. As a rule, the electrical resistivity of ordered alloys decreases with increasing degree of atomic

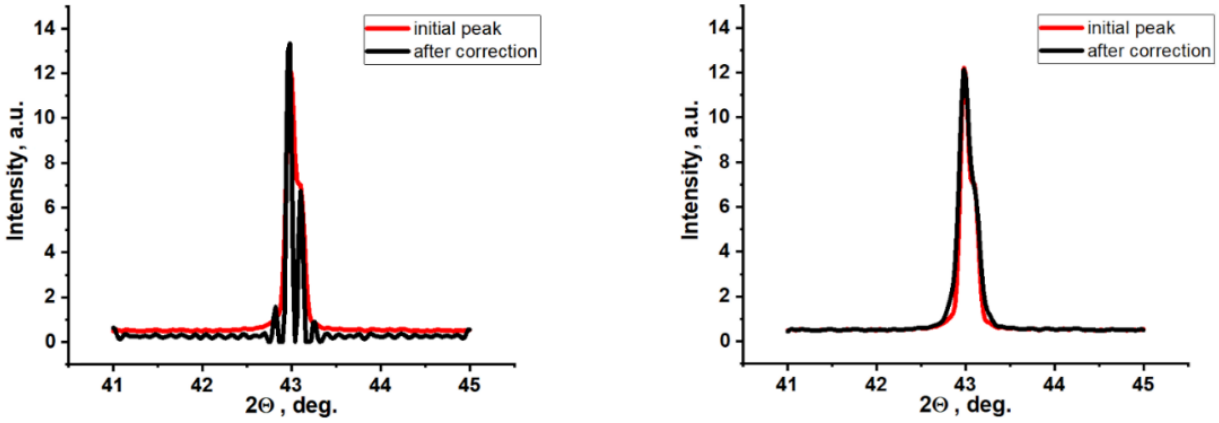

Fig. 3. (Color online) The instrumental broadening correction of the diffractogram obtained from the long-term annealed alloy: initial (111) peak is a superposition of four independent peaks (a); convolution of the solution in Fig. 3 a with the instrumental function (b).

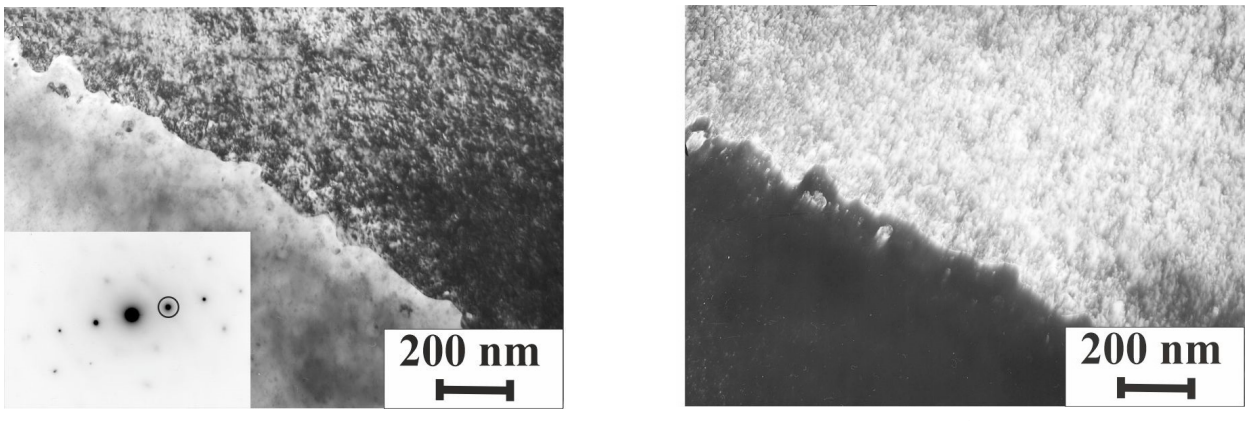

Fig. 4. Microstructure of the Cu-5.9 Pd alloy formed as a result of the long-term moderate-temperature annealing: bright-field image of a grain boundary (a); the insert shows SAED of the central portion in Fig. 4 a: the zone axis [110]; dark-field image of the microstructure Fig. 4 a in the reflection of the (111) type marked with symbol ○ in the insert in Fig. 4 a (b).

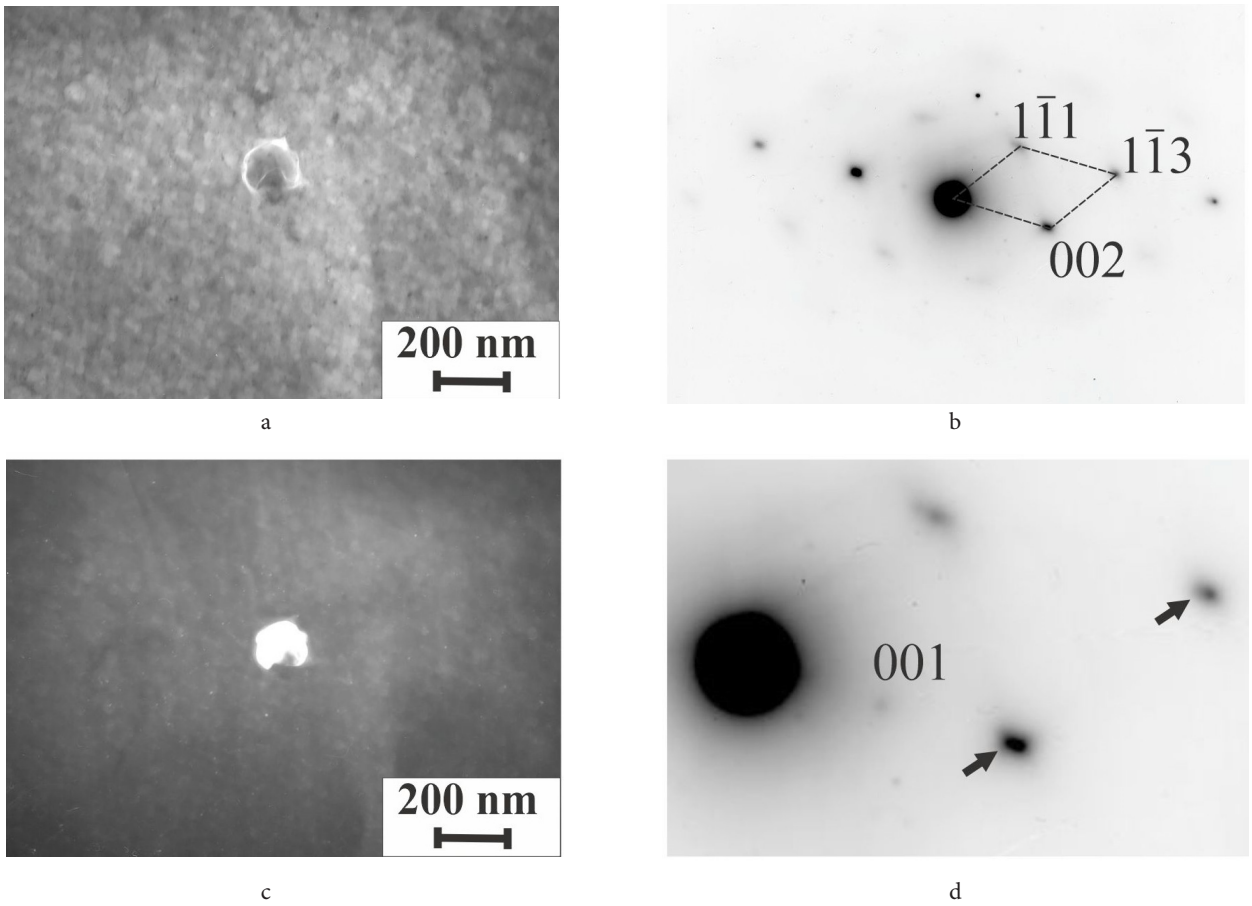

Fig. 5. Formation of a nuclei of ordered phase: bright-field image (a); SAED pattern from the central part of Fig. 5 a, with the zone axis [110] (b); dark-field image in the reflection of the (002) type (c); the central part of the SAED pattern shown in Fig. 5 b, arrows point at split reflections (d).

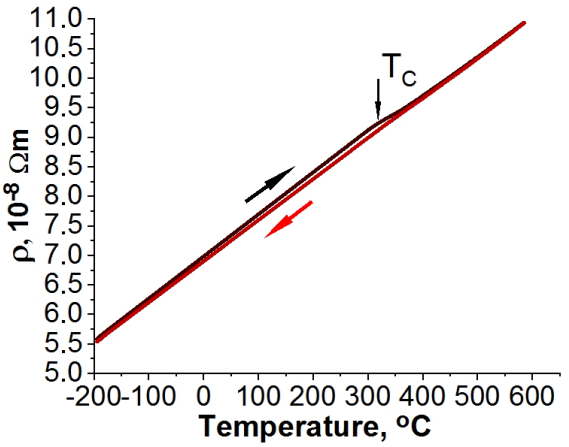

Fig. 6. (Color online) Temperature dependence of the electrical resistivity obtained during the heating and cooling of the Cu-5.9 Pd alloy annealed at 250°C for 2 months.

order [26]. It is due to the fact that the scattering of electrons is reduced in a crystalline lattice with a regular repeating of atoms of different nature composing the alloy lattice. However, decreasing of residual electrical resistivity during atomic ordering of the alloys in the vicinity of the Cu_3Pd stoichiometry is combined with simultaneously increasing their temperature coefficient of electrical resistivity [24]. In result of competition of these trends, after the formation of the $L1_2$ superstructure, the room-temperature value of the electrical resistivity of these alloys has to become higher [25]. After heating above the critical temperature of the order — disorder phase transition (T_c), the alloy is allowed only to be in the disordered state, and it is remained in this state after cooling down to room temperature due to a very low rate of the order-disorder transformation. According to the methodology suggested in [25], we assess the value of T_c to be for the alloy Cu-5.9 Pd approximately equal to 340°C (Fig. 6).

During this study, we carried out an additional experiment. A foil for the TEM-investigation made from the long-term annealed alloy was heated to 550°C and cooled down to the room temperature at the rate of 120°/hour. This heat treatment repeats completely the treatment that was carried out during the resistometric study in Fig. 6. A small step at ≈350°C in the temperature dependence of the electrical resistivity could be a response to structural transformation of some kind during heating. Therefore, it would be interesting to compare structural state of the sample before and after its heating.

Figure 7 presents the microstructure of the Cu-5.9 Pd alloy after additional heat treatment. A junction of three grains can be seen clearly in the TEM-image. Grain boundaries are straight, lamellar, and no precipitates are observed on them. The grains in Fig. 7 do not feature the heterogeneous contrast that was observed on the sample after long-term annealing (Fig. 4). It can be concluded that the additional heat treatment has led to changing of the structural state of the alloy.

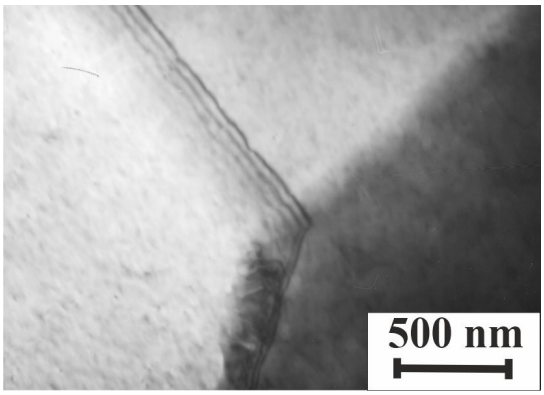

Fig. 7. Bright-field TEM image of long-term annealed Cu-5.9 Pd alloy sample which was additionally heated to 550°C and cooled to room temperature. A heating and cooling rate was 120°/hour.

4. Discussion

During this work, we studied the evolution of the microstructure and electrical properties under thermal treatment of the initially quenched Cu-5.9 Pd alloy samples only. Earlier, we had demonstrated that preliminary plastic deformation accelerated considerable the A1→$L1_2$ transformation in the diluted Cu-Pd alloys [15, 23]. However, at the same time, this causes certain issues in interpreting of the results obtained. For instance, wide peaks in the XRD-scans hinder identification of weak reflections of the ordered phase. The drop of electrical resistivity caused by recrystallization takes place within the same temperature interval, in which the response to the phase transformation is observed. Therefore, we have decided not to describe here the formation of structure and properties in the course of annealing of pre-deformed Cu-5.9 Pd alloy samples.

It should be mentioned that the rate of formation of new phase nuclei in the quenched alloy is low due to a small number of possible places of their nucleation. The rate of transformation is, as a rule, much higher in a pre-deformed alloy. In this case, nuclei can be formed in a heterogeneous manner, on various defects of the deformed structure. Moreover, movements of the boundary of growing grains in a non-recrystallized matrix is accompanied by a rearrangement of the dislocation structure, which increases significantly the rate of diffusion. This promotes accelerated formation of the new phase on the boundaries of recrystallized grains. These processes can lead to the increasing concentration of palladium on the dislocations and on the grain boundaries discovered in [13] during annealing of the pre-deformed Cu-7 Pd alloy. In turn, the coarse grains with ≈40 μm in size with minimum number of defects are observed in the structure of the quenched Cu-5.9 Pd alloy. As a result of the long-term annealing at 250°C, fine (less than 100 nm) nuclei of new phase appear in the quenched alloy both at the boundaries and in the volume of matrix grains due to thermal fluctuations of atoms or concentration variations (Figs. 4 and 5).

Based on all obtained results, it may be assumed that the ordered $L1_2$-phase may be formed in the Cu-5.9 Pd alloy as a result of the moderate annealing. The set of research methods we have used is quite sufficient for evaluation of structural state of any alloy. For instance, XRD-data and analysis of the temperature dependences of the electrical resistivity were used in works [27, 28] to study the processes of ordering in the Cu-Pd alloys.

The study showed that long-term annealing at 250°C resulted in considerable changes of the electrical properties of the Cu-5.9 Pd alloy (Fig. 6). We believe that only the nuclei formation of the ordered $L1_2$ phase can explain well these results. Indeed, the experiment in Fig. 6 shows very well that the temperature coefficient of electrical resistivity of the long-term annealed alloy is larger compared to that after heating above 350°C. It can be assumed that this value would be the temperature, at which the order-disorder phase transition occurs.

Moreover, we may, based on the resistometric study results, assess the critical temperature of the order-disorder phase transition (T_c) in the Cu-5.9 Pd alloy. According to the methodology suggested by T. Mitsui in [25], this temperature approximately corresponds to the top of the "step" on the temperature dependence of the electrical resistivity obtained in the course of the alloy heating. Previously, we used this method to estimate the temperature of the order-disorder phase transition in the Cu-8 Pd alloy [22]. The obtained result ($T_c \approx 380$°C) is in a good agreement with the Cu-Pd phase diagram in Fig. 1. As shown in Fig. 6, T_c for the Cu-5.9 Pd alloy is ≈340°C. Obviously, after heating above this temperature, the alloy may only be in the disordered state, and it remains in this state after cooling down to room temperature due to very low rate of the order-disorder transformation. This conclusion is in a good agreement with the TEM-observation result in Fig. 7. That is why the temperature coefficient of electrical resistivity of the alloy during heating is slightly higher. Since after our experiment with heating and cooling the alloy becomes disordered, electrical resistivity of the sample decreases (Fig. 6). This result is also in agreement with the annealing behavior of the ordered Cu-Pd alloys with $L1_2$ superstructure [24, 25].

The assumption about the possibility of A1-$L1_2$ phase transition in the Cu-5.9 Pd alloy is not in accordance with the phase diagram of the Cu-Pd system (Fig. 1), but it enables us to explain properly all abnormal features observed at the temperature dependence in Fig. 6. Based on the XRD-data, we have come to the conclusion that there are two new phases formed in the long-term annealed sample, i.e., palladium enriched and palladium depleted phases (Fig. 3). The presence of superstructure reflections from the particle indicates unambiguously the formation of an $L1_2$ superstructure in the Pd-rich areas (Fig. 5). It should be noted that during the TEM-investigations, we observed on many occasions some small round holes in the foil made of the annealed alloy. The annular crack around the particle in Fig. 5 a helps to understand the nature of origination of these holes. Redistribution of atoms that takes place as the new phase is formed leads to palladium depletion in certain areas of the alloy. Due to reduced corrosion resistance, such areas are the first to be pickled during electrolytic polishing. Consequently, it is easy for a Pd enriched particle of the new phase located within this area to fall out of the sample. The TEM-image in Fig. 5 a points out unambiguously to redistribution of palladium near the boundary of the particle generated during the long-term annealing of the Cu-5.9 Pd alloy.

5. Conclusion

In summary, we showed that long-term annealing at 250°C resulted in considerable changes of the microstructure and electrical properties of the Cu-5.9 Pd alloy. We believe that only the formation of the ordered $L1_2$ phase can explain well all obtained results. Moreover, we observed the ordered phase particle experimentally by the TEM method. The temperature of the order-disorder phase transition in the Cu-5.9 Pd alloy was estimated as $T_c \approx 340$°C. It can be concluded from our results that the two-phase (A1+$L1_2$) region is somewhat wider than it is depicted in the Cu-Pd phase diagram and this region must include compositions of the alloys with lower Pd contents (the temperature boundary of the A1↔ (A1+ $L1_2$) phase transition that was determined in our study is shown in Fig. 1). Of course, this presumption requires its further checking in other dilute Cu-Pd alloys annealed at the temperatures below 300°C for as long annealing periods as possible.

Acknowledgements. This work was carried out within the state assignment themes "Pressure" 122021000032-5. The TEM investigations were performed using the equipment of the Electron Microscopy Department of the Collective-Use Center, and X-ray diffraction studies were conducted on the equipment of the Collective-Use Center "Testing Center of Nanotechnologies and Advanced Materials" of the Institute of Metal Physics, Ural Branch, Russian Academy of Sciences.

References

1. A. A. Popov, Yu. V. Shubin, P. E. Plyusnin et al. J. Alloys Compd. 777, 204 (2019). Crossref
2. V. M. Ievlev, K. A. Solntsev, A. I. Dontsov, A. S. Prizhimov, S. V. Gorbunov, N. R. Roshan, S. V. Kannykin. Inorg. Mater. 56, 113 (2020). Crossref
3. M. A. Habib, A. Harale, S. Paglieri et al. Energy Fuels. 35, 5558 (2021). Crossref
4. V. M. Ievlev, A. I. Dontsov, V. I. Novikov et al. Russ. Metall. (Met.). 2018, 854 (2018). Crossref
5. V. V. Krisyuk, A. E. Turgambaeva, I. V. Mirzaeva et al. Vacuum. 166, 248 (2019). Crossref
6. O. S. Novikova, K. O. Lavrinova, A. E. Kostina. Inorg. Mater. 55 (2), 116 (2019). Crossref
7. C. Chang, F. Hung, T. Lui. J. Electron. Mater. 46 (7), 4384 (2017). Crossref
8. O. S. Novikova, A. Yu. Volkov. Johns. Matthey Technol. Rev. 58 (4), 195 (2014). Crossref
9. P. R. Subramanian, D. E. Laughlin. J. of Phase Equilibria. 12 (2), 231 (1991). Crossref
10. P. Huang, S. Menon, D. de Fontaine. J. of Phase Equilibria, 12 (1), 3 (1991). Crossref
11. P. P. Fedorov, Yu. V. Shubin, E. V. Chernova. Russ. J. Inorg. Chem. 66, 891 (2021). Crossref
12. A. E. Kostina, O. S. Novikova, A. V. Glukhov et al. Phys. Met. Metallogr. 123 (1), 37 (2022). Crossref
13. I. Markovic, S. Ivanov, U. Stamenkovic et al. J. Alloys Compd. 768, 944 (2018). Crossref
14. J. M. Vitek, H. Warlimont. Metall. Mater. Trans. A. 10, 1889 (1979). Crossref
15. A. Yu. Volkov, A. E. Kostina, E. G. Volkova et al. Phys. Met. Metallogr. 118 (12), 1236 (2017). Crossref
16. G. Ceder, D. de Fontaine, H. Dreysse et al. Acta metall. mater. 38 (11), 2299 (1990). Crossref
17. M. Li, C. Guo, C. Li. CALPHAD. 32, 439 (2008). Crossref
18. S. Barthlein, E. Winning, G. Hart et al. Acta Mater. 57, 1660 (2009). Crossref
19. F. Geng, J. R. Boes, J. R. Kitchin. CALPHAD. 56, 224 (2017). Crossref
20. A. A. Popov, A. D. Varygin, P. E. Plyusnin et al. J. Alloys Compd. 891, 161974 (2022). Crossref
21. A. V. Zadesenets, Yu. V. Shubin, S. V. Korenev. Mater. Today Commun. 31, 103247 (2022). Crossref
22. A. N. Tikhonov, V. Ya. Arsenin. Solution of Ill-Posed Problems (ed. V. H. Winston). Washington, Harper and Brace (1977) 258 p.
23. E. G. Volkova, O. S. Novikova, A. Yu. Volkov. IOP Conf. Ser.: Mater. Sci. Eng. 447, 012029 (2018). Crossref
24. K. Mitsui, M. Takahashi. Scr. Mater. 38 (9), 1435 (1998). Crossref
25. K. Mitsui. Philos. mag. B. 81 (4), 433 (2001). Crossref
26. F. E. Jaumot, A. Sawatzky. Acta Metall. 4 (2), 127 (1956). Crossref
27. T. Shiraishi. J. Japan Inst. Metals. 46 (3), 245 (1982).
28. K. Hisatsune, K. Hasaka, T. Morimura et al. J. Alloys Compd. 230, 94 (1995). Crossref